Energy 74 (2014) 331–339

Contents lists available at ScienceDirect

Energy

journal homepage: www.elsevier.com/locate/energy

Theoretical and experimental investigation of steam injected diesel engine with EGR

Görkem Kökkülünk [a, *], Adnan Parlak [a], Vezir Ayhan [c], İdris Cesur [c], Güven Gonca [b], Barış Boru [c]

[a] Yildiz Technical University, Marine Engineering Department, Besiktas, Istanbul, Turkey
[b] Yildiz Technical University, Naval Architecture and Marine Engineering Department, Besiktas, Istanbul, Turkey
[c] Sakarya University, Faculty of Technology, Sakarya, Turkey

ARTICLE INFO

Article history:
Received 28 December 2013
Received in revised form
27 May 2014
Accepted 25 June 2014
Available online 31 July 2014

Keywords:
Diesel engine
Steam
Emissions
Combustion model
EGR

ABSTRACT

Steam injection technique newly proposed with EGR (exhaust gas recirculation) is applied into a direct injection diesel engine to decrease NO_x emissions for the objective of reaching the new emission regulations. Experimental and combustion model as a theoretical methodology has been done. Steam injected diesel engine with EGR has been performed using a combustion model for 20% steam (S20) and 10% EGR (E10) ratios of fuel mass injected per cycle at full-load conditions. The results have been compared with S20 in terms of performance and NO, CO, CO_2, and HC emissions. In the experimental results, NO emissions decreased up to 48.3% at the condition of S20 + E10 when compared to S20 with the increase of 3.5% in SFC (specific fuel consumption). As a result, when the small deterioration in the SFC is tolerated, the presented study could be used as an essential tool by the real-engine designers.

1. Introduction

The maximum limits of emissions released from diesel engine were reduced by international regulations year after year. Future emission regulations such as MARPOL (International Convention for the Prevention of Pollution from Ships) Annex VI and EURO VI for the automotive engines, have forced the manufacturers to limited pollutant emissions, particularly NO_x emissions.

Methods commonly used to decrease NO_x emissions are water injection into the engine cylinder and EGR (exhaust gas recirculation) [1–5]. Nowadays, water injection method has become more popular. Water injection can be applied to diesel engines with different methods. These are direct water injection into cylinder, emulsification and fumigation methods. The aim of the water injection is to reduce the formation rate of NO_x emissions by decreasing local maximum temperatures in cylinder [2,3] and also this method improves atomization by increasing droplet micro explosions [6]. Consequently, it was observed that NO_x emissions reduce [2,7,8,42,43], HC and CO emissions and SFC (specific fuel consumption) increase [7,9,10] using water injection. However, one of the main drawbacks of water injection methods is that condensed water deteriorates the specification of lubrication oil and increases the wear rate of moving parts of engine [11].

Another method in order to control NO_x emissions is to inject water into the engine cylinder in the form of steam phase developed by Parlak et al. [12]. It is revealed that NO_x emissions decrease up to 33%, effective power increase up to 3% and SFC decreases up to 5% as a consequence of full-load conditions with steam injection. Moreover, the optimum ratio of the steam was found as 20% (S20) [12–14]. Murthy et al. [15] demonstrated that NO emissions diminish; soot emissions, thermal efficiency, effective power and SFC rise up at full-load tests when the solar generated steam is injected into diesel engine.

EGR is another technology to reduce NO_x emissions from diesel engines [11,16–20]. EGR reduces local temperatures in the cylinder owing to the less oxygen amount and the more heat capacity of CO_2 and H_2O in comparison to air; because of these effects of EGR, NO_x formation rate reduces [21]. Even though EGR reduces NO_x emissions, it affects the engine performance and moving parts of engine negatively causing contamination of lubricating oil [22]. As a result of EGR applications, NO_x emissions reduce significantly [11,17–24], HC emissions increase [22,23,25], smoke emissions decrease [24–26], CO emissions increase [22,23], SFC increases [23,27–30] and PM (particulate matter) emissions enhance [28,29]. In some studies, it is stated that HC emission decreases with internal EGR [11,41].

* Corresponding author. Tel.: +90 2123832936; fax: +90 2123832941.
E-mail address: gorkemkulunk@gmail.com (G. Kökkülünk).

http://dx.doi.org/10.1016/j.energy.2014.06.091
0360-5442/

There is no study investigating the effects of EGR on steam-injected diesel engines. Thus, in this work, an electronically controlled steam injection system coupled with EGR were applied into direct injection diesel engine to examine torque, effective power and efficiency, SFC, in-cylinder pressure and temperature, and NO, CO, CO_2 and HC emissions.

2. Materials and methods

2.1. Experimental set-up and methodology

The experiments were performed using a single cylinder, naturally aspirated and four-stroke Diesel engine. The engine specification and experimental set-up are shown in Table 1 and Fig. 1, respectively [1,31,32]. Method of Needham et al. [33] was used in order to determine the amount of CO_2 gas. EGR percentage is:

$$\text{EGR}\ (\%) = \frac{CO_{2(\text{intake\_manifold})} - CO_{2(\text{surroundings})}}{CO_{2(\text{exhaust\_manifold})}} \times 100 \tag{1}$$

where $CO_{2(\text{surroundings})}$ is the reference CO_2 percentage in surroundings. In this study, this value was neglected owing to being 0.03% in the literature. EGR ratios were determined with a volume ratio of CO_2 value. In the experiments, 10%, 20% and 30% EGR ratios were carried out.

Experiments were carried out at variable speeds such as 1200, 1400, 1600, 1800, 2000, 2200 and 2400 rpm at full-load conditions [1,32].

Table 2 illustrates the errors in parameters and total uncertainties with 95% confidence interval.

In this study, MRU Spectra 1600 L type and Bilsa Mod gas analyzers were used so as to measure the exhaust gases. Before experiments, emission devices were calibrated. Table 3 illustrates the technical data of MRU 1600 L emission device [1,31,32].

Meanwhile, Table 4 shows the analysis of MAPE (mean absolute percentage error), RMSE (root mean square error) and standard deviation values of theoretical and experimental data [1,31,32].

2.2. The simulation model

In the theoretical model, fuel injected engine is performed by using two-zone combustion model [36,44,45]. In the cylinder, the equation of the energy conservation in differential form could be expressed as [34,44,45]:

$$m\frac{du}{d\theta} + u\frac{dm}{d\theta} = -\frac{dQ_b}{d\theta} - \frac{dQ_u}{d\theta} - P\frac{dV}{d\theta} + \frac{dm_{fi}}{d\theta}h_{fi} - \frac{dm_l}{d\theta}h_l \tag{2}$$

The mass balance inside the cylinder can be expressed as:

$$m = m_a + m_{fi} \tag{3}$$

where m_a and m_{fi} are the masses of the air and injected fuel, respectively. If Eq. (3) is written in differential form, it becomes:

$$\frac{dm}{d\theta} = \frac{dm_a}{d\theta} + \frac{dm_{fi}}{d\theta} \tag{4}$$

The air and injected fuel rates changing with crank angle within the cylinder are expressed, respectively, as:

$$\frac{dm_a}{d\theta} = \frac{-\dot{m}_l/\omega}{1+\phi F_{st}} = \frac{-Cm_a}{\omega} \tag{5}$$

$$\frac{dm_{fi}}{d\theta} = \frac{1}{\omega}\left(\dot{m}_{fi} - \frac{\dot{m}_l \phi F_{st}}{1+\phi F_{st}}\right) = \frac{\dot{m}_{fi} - Cm_{fi}}{\omega} \tag{6}$$

where $\dot{m}_1$, φ and F_s are the time-dependent gas leak rate, the equivalence ratio, and the stoichiometric fuel–air ratio by mass, respectively. $\dot{m}_{fi}$ is the time-dependent fuel injected rate and can be expressed as:

$$\dot{m}_{fi} = \dot{x}_i m_{fi} \tag{7}$$

where m_{fi} and x_i are the total mass of the fuel to be injected and fraction rate of the total injected fuel mass which can be given as:

$$m_{fi} = \phi F_{st}(1 - \text{RGF})m_a \tag{8}$$

$$\dot{x}_i = \frac{\omega}{\theta_{di}\Gamma(n)}\left(\frac{\theta - \theta_{si}}{\theta_{di}}\right)^{n-1} \exp\left[\frac{-(\theta - \theta_{si})}{\theta_{di}}\right] \tag{9}$$

where $\Gamma(n)$ is the gamma function [34], θ_{di} is a parameter of injection duration and θ_{si} is the start of fuel injection.

The values of n have been taken for the diesel engine with close chamber as 3.5 in accordance with the values that have been taken from the engine manufacturer.

Differential equation systems, which have been used in the calculation of the processes that consist of those during the period from the beginning of the compression to the end of the expansion process, are given in Eq. (15) [36–45].

The time (crank angle)-dependent expressions of pressure, burned and unburned gas temperatures, work, heat leak and heat loss are given, respectively, as:

$$\frac{dP}{d\theta} = \frac{\dfrac{C}{\omega}\left(\dfrac{V}{m}+\dfrac{\vartheta_1}{C_{p,b}T_b}\left(\left(x^2-x\right)(h_b-h_u)\right)\right)+\dfrac{h_{tr}}{\omega m}A_{cyl}\left(\sqrt{x}\dfrac{\vartheta_1}{C_{p,b}T_b}T_{bw}+(1-\sqrt{x})T_{uw}\dfrac{\vartheta_2}{C_{p,u}T_u}\right)+\left(\dfrac{\vartheta_1}{C_{p,b}T_b}(h_b-h_u)-(v_b-v_u)\right)\dfrac{dx}{d\theta}+\dfrac{1}{m}\dfrac{dV}{d\theta}}{x\left(\dfrac{\vartheta_1}{C_{p,b}T_b}+\dfrac{\vartheta_3}{P}\right)+(1-x)\left(\dfrac{\vartheta_2^2}{C_{p,u}T_u}+\dfrac{\vartheta_4}{P}\right)} \\ +\dfrac{\left(\dfrac{\vartheta_1}{mC_{p,b}T_b}(xh_b-(1-x)h_u)-H_u-\dfrac{V}{m^2}\right)\dfrac{dm_{fi}}{d\theta}+(1-x)\left(\dfrac{\vartheta_1}{C_{p,b}T_b}\left(-T_u\dfrac{ds_u}{d\theta}+P\dfrac{dv_u}{d\theta}+\dfrac{du_u}{d\theta}\right)-\dfrac{dv_u}{d\theta}+\dfrac{\vartheta_2}{C_{p,u}}\dfrac{ds_u}{d\theta}\right)\dfrac{d\phi}{d\theta}+x\left(\dfrac{\vartheta_1}{C_{p,b}T_b}\left(P\dfrac{dv_b}{d\theta}+\dfrac{du_b}{d\theta}\right)-\dfrac{dv_b}{d\theta}\right)\dfrac{d\phi}{d\theta}}{x\left(\dfrac{\vartheta_1}{C_{p,b}T_b}+\dfrac{\vartheta_3}{P}\right)+(1-x)\left(\dfrac{\vartheta_2^2}{C_{p,u}T_u}+\dfrac{\vartheta_4}{P}\right)} \tag{10}$$

where m_1 is leak mass and m_{fi} is mass of injected fuel; h_{fi} and h_1 are enthalpies of fuel injected and leak mass, respectively. The first term on the left-hand side of the equation is the internal energy rate and the second term is the mass rate depending on the crank angle.

where x, H_u, A_{cyl} are the burning fraction, lower heating value of fuel and heat transfer area of the cylinder, respectively. $C_{p,b}$, $C_{p,u}$, v_b, v_u, s_b, s_u, h_b and h_u are specific heat at constant pressure, specific volume, specific entropy and specific enthalpy for the burned and unburned zones, respectively.

Table 1
Engine specification.

Engine type	Super star
Bore [mm]	108
Stroke [mm]	100
Cylinder number	1
Stroke volume [dm^3]	0.92
Power, 1500 rpm [kW]	13
Injection pressure [bar]	175
Injection timing [crank angle]	35
Compression ratio	17
Maximum speed [rpm]	2500
Cooling	Water
Injection	Direct injection

Table 2
The errors in parameters and total uncertainties with 95% confidence interval [1,30,31].

Parameters	Systematic errors, ±
Load, N	0.1
Speed, rpm	1.0
Time, s	0.1
Temperature, °C	1
Fuel consumption, g	0.5
	Total uncertainty, %
Effective efficiency, %	1.5
Effective power, kW	1.1

Hohenberg [35] gives the coefficient of the heat transfer (h_{tr}) as follows:

$$h_{tr} = C_1 V^{-0.06} P^{0.8} (xT_b + (1-x)T_u)^{-0.4} \left(\bar{S}_p + C_2\right)^{0.8} \quad (11)$$

where $\bar{S}_p$ is the mean piston velocity in m/s, $C_1 = 130$ and $C_2 = 1.4$. Sitkei [46] correlation is used to calculate ignition delay and it is written as follows:

$$\tau_{id} = 0.5 + 0.1332 P^{-0.7} e^{3.92782/T} + 4.637 P^{-1.8} e^{3.92782/T} \quad (12)$$

where P and T are, respectively, average temperature and pressure during the ignition delay.

Dual Wiebe function states the burn fraction and x versus crank angle are used to express the heat release from combustion and determined as follows [36,44,45]:

$$x = a_v \left[Q_{pre} \left(1 - e^{-a_v (\theta/\theta_{pre})^{(m_{pre}+1)}}\right) + Q_{dif} \left(1 - e^{-a_v (\theta/\theta_{dif})^{(m_{dif}+1)}}\right)\right] \quad (13)$$

where Q_{pre} and Q_{dif} are heat release rate percentages of premixed and diffusive combustion, respectively. x is 0 at the beginning of the combustion and x becomes 1 at the end of the combustion. It can be rewritten by differentiating with respect to crank angle:

$$\frac{dx}{d\theta} = a_v \left[\frac{Q_{pre}}{\theta_{pre}} (m_{pre}+1) \left(\frac{\theta}{\theta_{pre}}\right)^{m_{pre}} e^{-a_v (\theta/\theta_{pre})^{(m_{pre}+1)}} + \frac{Q_{dif}}{\theta_{dif}} (m_{dif}+1) \left(\frac{\theta}{\theta_{dif}}\right)^{m_{dif}} e^{-a_v (\theta/\theta_{dif})^{(m_{dif}+1)}} \right] \quad (14)$$

$$\theta = \theta_r - \theta_b \quad (15)$$

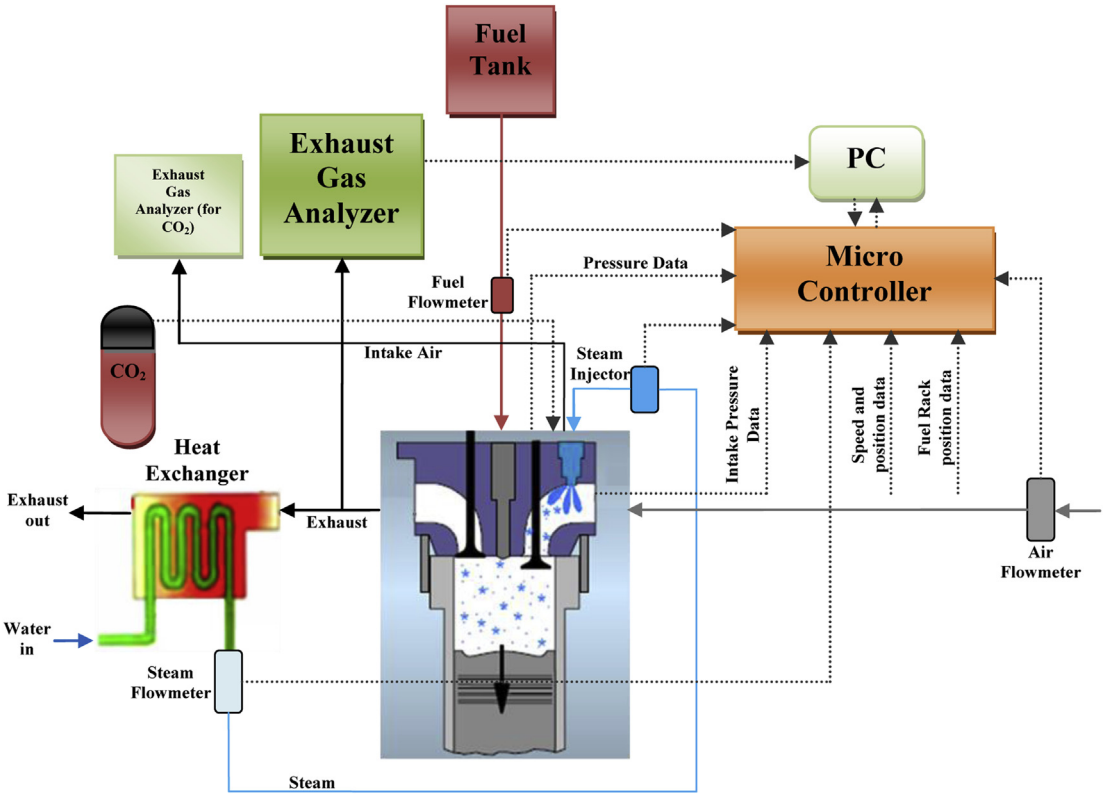

Fig. 1. Experimental set-up.

Table 3
Technical data of MRU 1600 L emission device [1,30,31].

Measured parameters	Unit	Measuring range	Measured precision
CO	%	0–15.0	±0.06% or ±%5 of measured value
CO_2	%	0–20.0	±0.5% or ±%5 of measured value
HC (*n*-hexane)	ppm	0–20,000	±12 ppm or ±%5 of measured value
NO	ppm	0–2000	±5 ppm or ±%5 of measured value

where θ_r and θ_b are reference crank angle and start angle of combustion, respectively; a_v, m_{pre}, θ_{pre}, m_{dif}, θ_{dif} are Wiebe constants in the premixed and diffusive combustion conditions.

Extended Zeldovich mechanism is used in order to calculate NO emissions considering 10 combustion products involving (CO_2, H_2O, N_2, O_2, CO, H_2, H, O, OH, NO) [31,32,37]. In this work, the ECP code proposed by Olikara and Borman [38] is developed by adding steam injection and CO_2 into the reactants because CO_2 is the dominant gas in exhaust gases and it can be used as simplification in the computations. The combustion reaction is expressed as below:

$$\varepsilon\phi C_\alpha H_\beta O_\gamma N_\delta + (0.21O_2 + 0.79N_2) + xH_2O + yCO_2 \rightarrow \nu_1 CO_2 + \nu_2 H_2O + \nu_3 N_2 + \nu_4 O_2 + \nu_5 CO + \nu_6 H_2 + \nu_7 H + \nu_8 O + \nu_9 OH + \nu_{10} NO$$

where ε is molar fuel–air ratio, which is given as [32,34]:

$$\varepsilon = \frac{0.21}{\alpha + 0.25\beta - 0.5\gamma} \tag{16}$$

The x constant in the reactants is the mole fraction of injected steam and could be obtained as:

$$x = \frac{Y_{\%} M_{air}}{M_{ste}} \tag{17}$$

where M_{air} and M_{ste} are molecular weights of the air and steam, respectively. $Y_{\%}$ is the proportion of the steam mass to the air mass and determined as below:

$$Y_{\%} = \frac{m_{ste}}{m_{air}} \tag{18}$$

The y constant in the reactants is mole fraction of EGR (CO_2) and may be obtained as:

Table 4
Analysis of MAPE, RMSE and standard deviation of theoretical and experimental data [1,30,31].

	RMSE	MAPE	Standard deviation
Effective power	0.000002	0.0001	0.0017
Effective efficiency	0.000023	0.0001	0.0052
NO	0.083800	0.0006	0.2977

Table 5
Reactions of NO formation [32,39].

No.	Reaction	Forward/backward		
		A_A (cm^3/mol s)	B_A	E_A (kcal/mol K)
1	$N_2 + O \leftrightarrow NO + N$	$7.6 \times 10^{13}/1.6 \times 10^{13}$	0/0	−38,000/0
2	$O_2 + N \leftrightarrow NO + O$	$6.4 \times 10^{09}/1.5 \times 10^{09}$	0/0	−3150/−19,500
3	$OH + N \leftrightarrow NO + H$	$4.1 \times 10^{13}/2 \times 10^{14}$	0/0	0/−23,650

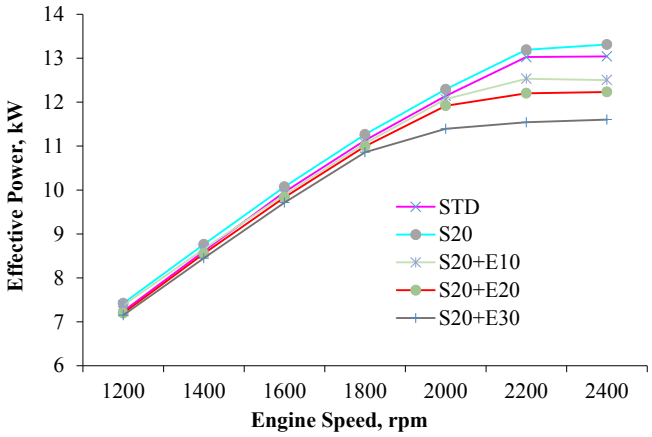

Fig. 2. Experimental results of effective power [1].

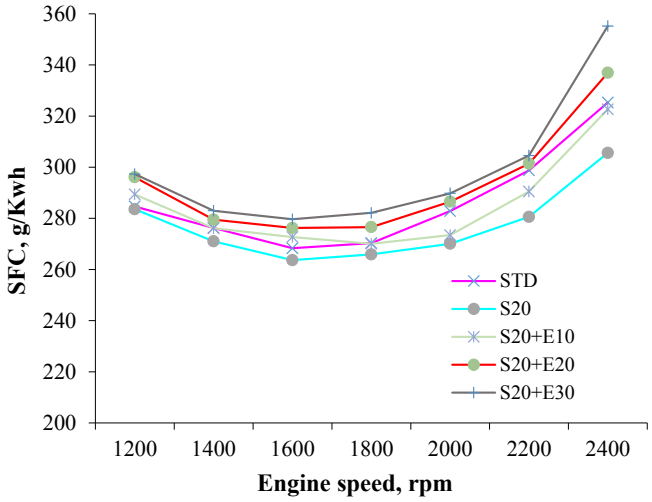

Fig. 3. Experimental results of SFC [1].

$$y = \frac{Z_{\%} M_{air}}{M_{CO_2}} \tag{19}$$

where M_{CO_2} is the molecular weight of CO_2. $Z_{\%}$ is the ratio of the CO_2 mass to the air mass and expressed as:

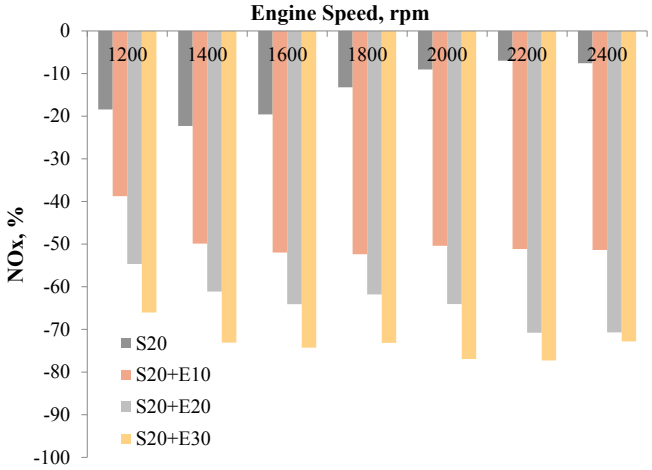

Fig. 4. Experimental results for NO_x emissions [1].

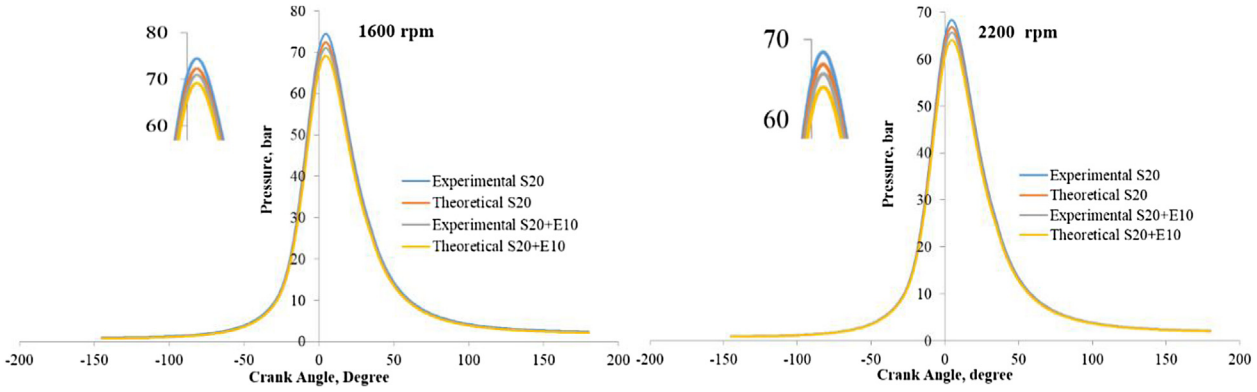

Fig. 5. Comparison of theoretical and experimental data of in-cylinder pressure.

$$Z_{\%} = \frac{m_{CO_2}}{m_{air}} \tag{20}$$

The reaction steps of NO formation may be seen in Table 5.
The rate constant is given as below:

$$k = A_A T^{B_A} e^{E_A/T} \tag{21}$$

The rate of NO formation [mol cm^{-3} s^{-1}] is [31,32,36,37]:

$$\frac{d[NO]}{dt} = \frac{2R_1(1-a^2)}{1+\frac{aR_1}{R_2+R_3}} \tag{22}$$

where $\alpha = [NO]/[NO]_e$ and $[\ ]_e$ denotes equilibrium concentration. The other constants is given in Eq. (22) are:

$$R_1 = k_{+1}[N_2]_e[O_2]_e = k_{-1}[NO]_e[N]_e \tag{23}$$

$$R_2 = k_{+2}[O_2]_e[N]_e = k_{-2}[NO]_e[O]_e \tag{24}$$

$$R_3 = k_{+3}[OH]_e[N]_e = k_{-3}[NO]_e[H]_e \tag{25}$$

3. Results and discussion

In this work, a verified combustion model [31,32,36] is used to examine the influences of steam-injected diesel engine with EGR on performance and emissions. Figs. 2–4 show the variations of effective power, specific fuel consumption (SFC) and NO_x emissions depending on various EGR ratios and for fixed steam ratio of 20% compared to those of standard diesel. It seems from Fig. 4 that NO_x emissions decrease as the EGR ratio increases. However, the increase in EGR ratio leads to increase SFC and decrease effective power drastically as can be seen from Figs. 2 and 3. Thus, 20% steam (S20) and 10% EGR ratios (S20 + E10) are only used in the present study as NO_x emissions are reduced significantly without important penalty on SFC and effective power.

3.1. Performance parameters

3.1.1. In-cylinder pressure

The comparison of the in-cylinder pressures of theoretical and experimental results at full-load tests is demonstrated in Fig. 5. It is found that the results of theoretical model are very close to the experimental data.

3.2. Engine effective parameters

3.2.1. Engine torque

Fig. 6 shows the comparison of theoretical and experimental results of torque. It is observed from the figure, steam injection increases the engine torque. However, according to experimental results, torque reduces at all engine speeds with S20 + E10. Maximum torque obtained is found as 60.2 N m and 59.4 N m at 1600 rpm with S20 and S20 + E10, respectively. While the maximum reduction in torque is 6.1% at 2400 rpm; the lowest decrease is 0.6% at 1200 rpm. The reason of deterioration in torque can be explained with the higher specific volume of exhaust gases

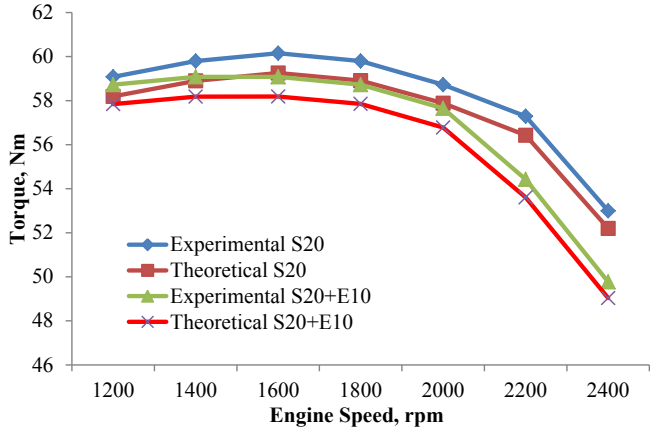

Fig. 6. Comparison of theoretical and experimental data of torque.

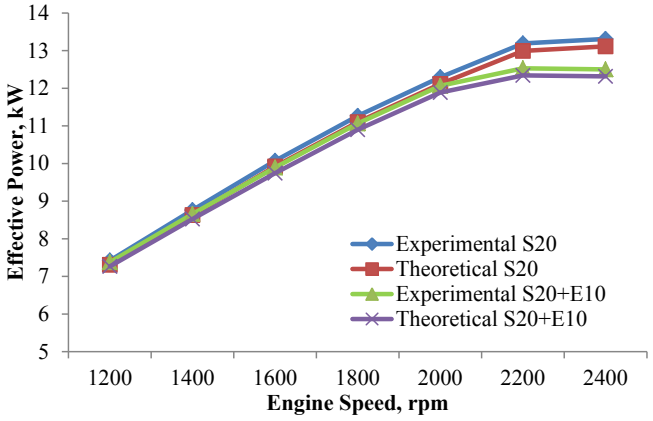

Fig. 7. Comparison of theoretical and experimental data of effective power.

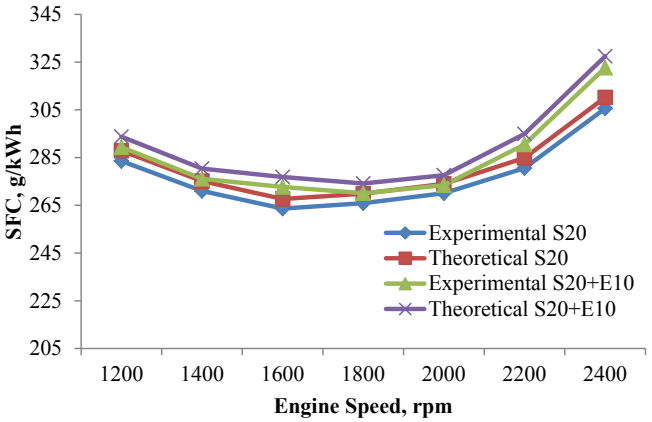

Fig. 8. Comparison of theoretical and experimental data of SFC.

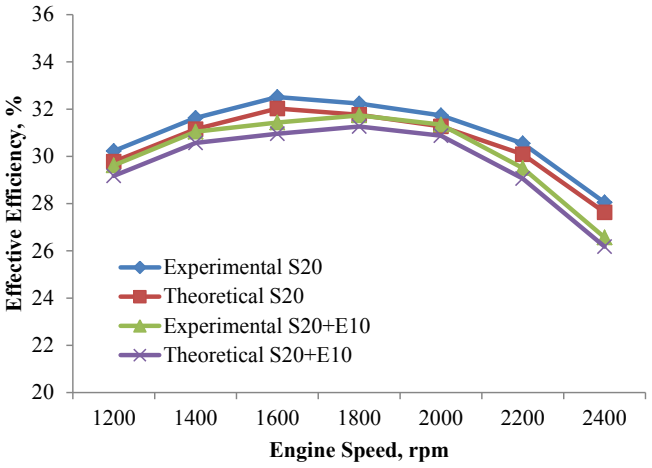

Fig. 9. Comparison of theoretical and experimental data of effective efficiency.

entering into the cylinder. Higher specific volume also leads to a decreased volumetric efficiency and leads to a decreased oxygen concentration in the cylinder. Thus all these factors contribute to the effective power reduction in case of EGR application.

3.2.2. Effective power

Fig. 7 shows the comparison of the theoretical and experimental data of effective power. It is clear that torque, effective power also decreases at all engine speeds with S20 + E10. The maximum effective power at 2400 rpm with S20 is 13.3 kW and 12.5 kW, respectively. Compared to the standard torque values, the highest change is 6.1% at 2400 rpm, the lowest change is 0.6% at 1200 rpm. The reason which causes to decrease engine torque, also it affects the effective power in the same way.

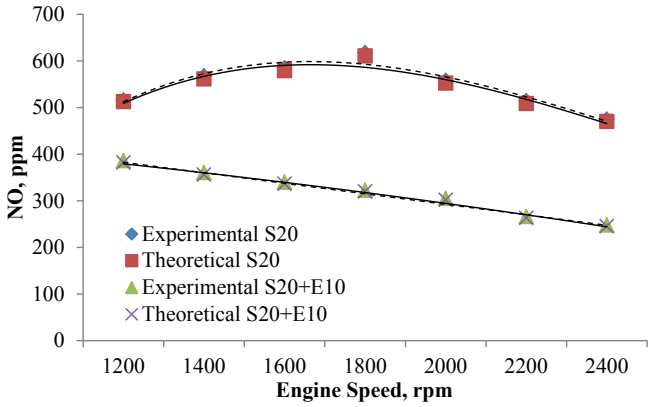

Fig. 11. Comparison of theoretical and experimental data of NO emissions.

3.2.3. Specific fuel consumption and effective efficiency

In Fig. 8, theoretical and experimental results of SFC are obtained comparatively. It is seen from the figure that SFC increases at all engine speeds with S20 + E10. The lowest SFC is 263.7 g/kWh at 1600 rpm and 270.1 g/kWh at 1800 rpm with S20 and S20 + E10, respectively. The highest increase is 5.6% at 2400 rpm, the minimum change is 1.2% at 2000 rpm in SFC, according to steam injected diesel engine. Fig. 9 shows theoretical and experimental results of effective efficiency. The decrease rates of effective efficiency are found same as SFC.

Also an increment is seen in SFC. The most possible reason of this increment is the worsening in volumetric efficiency of the engine as the specific volume of CO_2 is higher when compared to that of atmospheric air. If the cold EGR is used, the deterioration in the performance and the penalty of SFC can be minimized.

3.3. Emission parameters

3.3.1. In-cylinder temperature and NO formation

The comparison of in-cylinder temperatures of theoretical and experimental results at full-load tests with respect to engine speed is expressed in Fig. 10. The theoretical model has good agreement

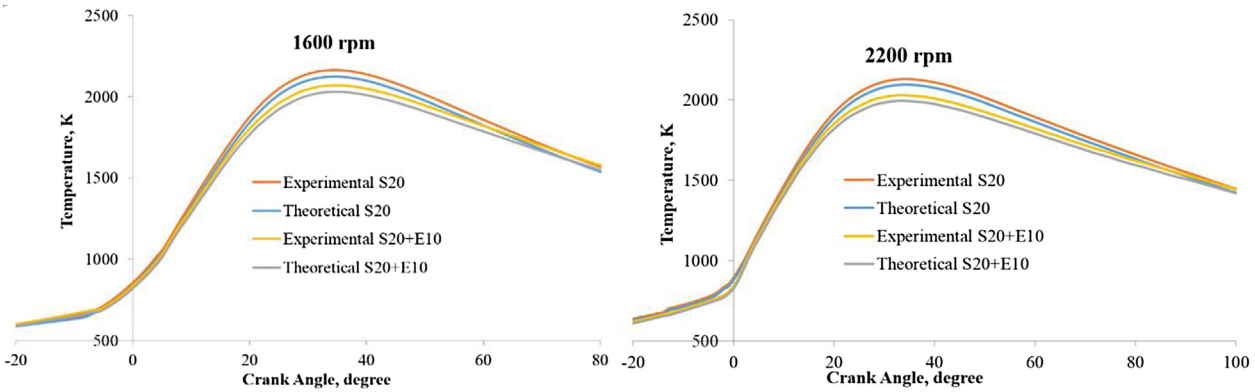

Fig. 10. Comparison of theoretical and experimental data of cylinder temperature.

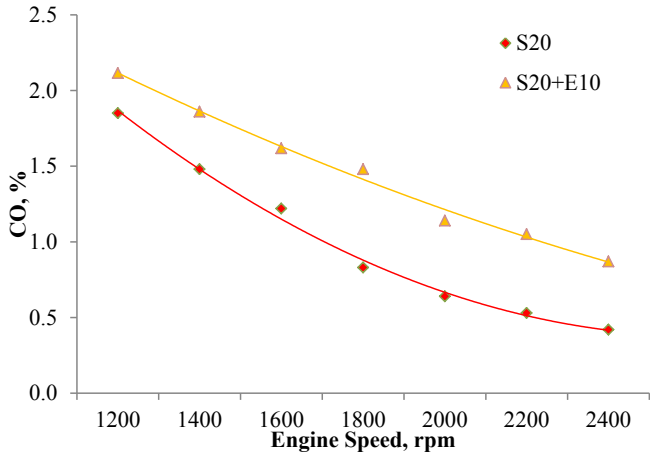

Fig. 12. Comparison of CO emissions of standard and steam injected diesel engines.

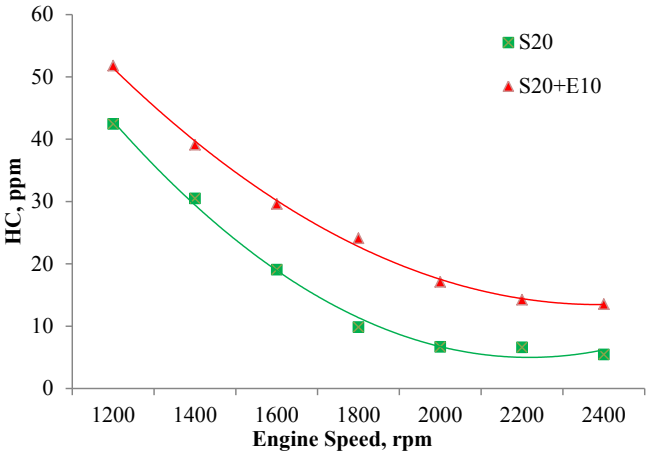

Fig. 14. Comparison of HC emissions of standard and steam injected diesel engines.

with experimental results. The influences of steam injection with EGR on in-cylinder gas temperature are clearly shown in the figure.

It is well known in the literature that rate of NO formation changes with respect to combustion temperature and combustion duration [40]. Hence, if the steam is injected into the intake manifold, maximum combustion temperatures decrease in comparison with that of standard diesel engine.

Fig. 11 gives the comparison of theoretical and experimental results of NO emissions. It can be observed from the figure, steam injection causes to reduce NO emissions whilst the maximum combustion temperatures reduce.

The NO emission formation reduces at all engine speeds with S20 + E10. The minimum NO is 248 ppm at 2400 rpm. The highest change is 48.3% at 2200 rpm and the lowest change is 25.2% at 1200 rpm.

3.3.2. CO and CO_2

Fig. 12 compares CO emissions of S20 with the S20 + E10. The CO emissions deteriorated with EGR ratios compared to those of S20 at all engine speeds. Besides, it is observed that the increase in the emission is within the limits of uncertainty when considering the measurement accuracy. Besides, in the experiments, considering 99% purity CO_2 gas is routed into intake manifold, the increase in CO emissions is in a normal rate. The minimum CO emission is 0.42% and 0.87% at 2400 rpm with S20 and S20 + E10, respectively.

Fig. 13 shows the comparison of the CO_2 emissions. The CO_2 emissions increase with optimum steam and EGR ratios at all the engine speeds. Furthermore, in the experiments, considering 99% purity CO_2 gas is introduced into intake manifold. Thus, one of the reasons of the increase in CO_2 emissions is to introduce CO_2 gas during inlet period. Another reason can be explained with poor combustion efficiency were in a normal rate. The minimum CO_2 emission is 10.2% and 12.7% at 2400 rpm for S20 and S20 + E10, respectively. In conclusion, CO_2 emissions increase because SFC increases with the steam injection as can be seen from Fig. 8.

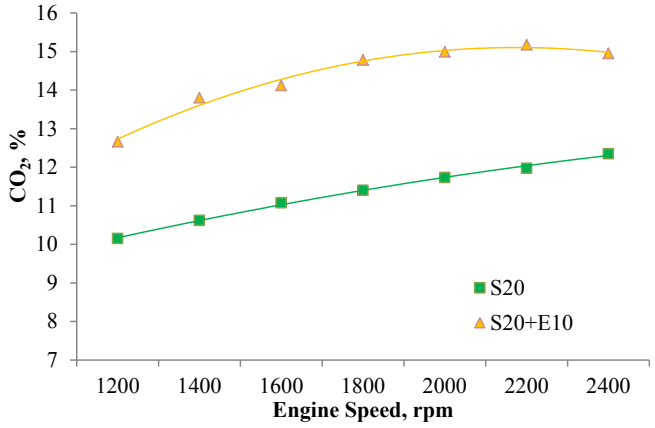

Fig. 13. Comparison of CO_2 emissions of standard and steam injected diesel engines.

3.3.3. HC

The comparison of HC emissions is illustrated in Fig. 14. The HC emissions increase with optimum steam and EGR ratios at all engine speeds. However, it is seen that the changes in the emission values of S20 and S20 + E10 diesel engines are within the limits of uncertainty when considering measurement accuracy. The minimum HC emission is 5.5 ppm and 13.5 ppm at 2400 rpm of S20 and S20 + E10.

4. Conclusion

In this work, the influences of steam injection technique with EGR on performance and emissions have been examined and modeled by a verified combustion model. The simulation results have been compared with the experimental data.

It is observed from the results that there is a reduction in NO emissions significantly and also NO emissions reduced with raising the EGR ratio. NO_x emissions with minimum loss in fuel economy are found with 10% EGR ratio and that could be favorable in a trade-off between CO, NO_x and HC emissions with little economy penalty.

It is clear that SFC increases at all engine speeds with S20 + E10. The optimum point is found at 2000 rpm with 1.2% increase in SFC and 45.3% decrease in NO emissions considering NO and SFC. Using high levels of EGR (30% EGR) has the beneficial effect of lowering the flame temperature, which leads to low NO_x emissions of 77.3% with the penalty on SFC of 9.2%.

As a result, steam injection with EGR gives good results in NO emissions at all speeds with little increase in SFC. However, the increase of SFC can be potentially minimized or improved if the cooled EGR is applied in the future study.

Hence, the presented study may be especially carried out in the marine engine applications to decrease NO_x emissions as a leading study taking into account the influences of steam injection with EGR into the engine cylinder. It can be concluded that the application of EGR on steam-injected diesel engine has a potential to meet MARPOL Annex VI Tier III in marine diesel engines.

Acknowledgement

This study was supported by TUBITAK 1001 Project (Project no. 111M065) and Yildiz Technical University (YTU) Scientific Research Project Coordination (BAPK) (Project no. 2011-10-02-KAP02). Thanks to TUBITAK and YTU BAPK for the financial support.

Nomenclature

EGR	Exhaust gas recirculation
SFC	Specific fuel consumption
DI	Direct injection
S20 + E10	20% Steam injection and 10% EGR
RGF	Residual gas fraction
m_1	Leak mass, g
m_{fb}	Mass of burned fuel, g
h_1	Enthalpy of combustion products, kJ/kg
C	Dimensionless constant
C_p	Specific heat of constant pressure of air fuel mixture, kJ/kg K
m_f	Total mass of the injected fuel, g
x_b	The rate of the total burned fuel mass to total mass of injected fuel
F_{st}	Stoichiometric fuel–air ratio by mass
Δh	Combustion enthalpy, kJ/kg
M_f	Molecular weight of fuel, kg/kmol
P_i	Injection pressure of fuel, bar
v_f	Specific volume of fuel, cm^3/g
A_{cyl}	Heat transfer area of cylinder, cm^2
T	Temperature of the in-cylinder gas zone, K
T_w	Temperature of the cylinder walls, K
h_{tr}	Heat transfer coefficient
p	In-cylinder pressure, bar
S_p	Mean piston velocity, m/s
v	Specific volume, cm^3/g
j	Ratio of half stroke to rod length
m_a	Mass of air, g
m_{fi}	Mass of injected fuel, g
ε	Molar fuel–air ratio
φ	The equivalence ratio
$\Gamma(n)$	Gamma function
θ	Instant crank angle, °
θ_{di}	Injection duration, °
θ_{si}	Start of fuel injection, °
θ_{db}	Burning duration, °
θ_{sb}	Start of burning, °
ω	Angular velocity, 1/rad

References

[1] Kökkülünk G, Parlak A, Ayhan V, Cesur I. Investigation of steam injection with exhaust gas recirculation (EGR) on a diesel engine. In: Third international conference on urban sustainability, cultural sustainability, green development, green structures and clean cars (USCUDAR '12), Barcelona; 2012. pp. 41–6.
[2] Samec N, Breda K, Dibble RW. Numerical and experimental study of water/oil emulsified fuel combustion in a diesel engine. Fuel 2002;81:2035–44.
[3] Bedford F, Rutland C, Dittrich P, Raab A, Wirbelit F. Effects of direct water injection on DI diesel engine combustion. SAE paper 2000-01-2938.
[4] Park JW, Huh KY, Lee JH. Reduction of NO_x, smoke and brake specific fuel consumption with optimal injection timing and emulsion ratio of water-emulsified diesel. P I MechEng D-J Aut 2001;215:83–93.
[5] Armas O, Ballesteros R, Martos FJ, Agudelo JR. Characterization of light duty diesel engine pollutant emissions using water-emulsified fuel. Fuel 2005;84:1011–8.
[6] Dryer FL. Water addition to practical combustion systems – concepts and applications. Symp Int Combust 1977;16:279–95.
[7] Lin CY, Wang KH. Diesel engine performance and emission characteristics using three-phase emulsions as fuel. Fuel 2004;83:537–45.
[8] Tauzia X, Maiboom A, Shah SR. Experimental study of inlet manifold water injection on combustion and emissions of an automotive direct injection diesel engine. Energy 2010;35:3628–39.
[9] Abu-Zaid M. Performance of single cylinder, direct injection diesel engine using water fuel emulsion. Energ Convers Manage 2004;45:697–705.
[10] Alahmer A, Yamin J, Sakhrieh A, Hamdan MA. Engine performance using emulsified diesel fuel. Energ Convers Manage 2010;51:1708–13.
[11] Abd-Alla GH, Soliman HA, Badr OA, Abd-Rabbo MF. Effects of diluent admissions and intake air temperature in exhaust gas recirculation on the emissions of an indirect injection dual fuel engine. Energ Convers Manage 2001;42:1033–45.
[12] Parlak A, Ayhan V, Üst Y, Şahin B, Cesur I, Boru B, et al. New method to reduce NO_x emissions of diesel engines: electronically controlled steam injection system. J Energ Inst 2012;85:135–9.
[13] Parlak A, Ayhan V, Şahin B, Cesur İ, Boru B, Kökkülünk G. The effects of the new developed electronic controlled steam injection system on NO_x emissions of a single cylinder diesel engine. In: Thirteenth international conference maritime transport and infrastructure, Riga; 2011.
[14] Cesur İ, Parlak A, Ayhan V, Gonca G, Boru B. The effects of electronic controlled steam injection on spark ignition engine. Appl Therm Eng 2013;55:61–8.
[15] Murthy YVVS, Sastry GYK, Satyanaryana MRS. Experimental investigation of performance and emissions on low speed diesel engine with dual injection of solar generated steam and pongamia methyl ester. Ind J Sci Technol 2011;4:29–33.
[16] Kosmadakis GM, Rakopoulos CD, Demuynck J, De Paepe M, Verhelst S. CFD modeling and experimental study of combustion and nitric oxide emissions in a hydrogen-fueled spark-ignition engine operating in a very wide range of EGR rates. Int J Hydrogen Energy 2012;37:10917–34.
[17] Heffel JW. NO_x emission reduction in a hydrogen fuelled internal combustion engine at 1500 rpm using exhaust gas recirculation. Int J Hydrogen Energy 2003;28:901–8.
[18] Selim MYE. Effect of exhaust gas recirculation on some combustion characteristics of dual fuel engine. Energy Convers Manage 2003;44:707–21.
[19] Zheng M, Reader GT, Hawley JG. Diesel engine exhaust gas recirculation—a review on advanced and novel concept. Energy Convers Manage 2004;45:883–900.
[20] Pirouzpanah V, Saray KR, Sohrabi A, Niaei A. Comparison of thermal and radical effects of EGR gases on combustion process in dual fuel engines at part loads. Energy Convers Manage 2007;48:1909–18.
[21] Angrill O, Geitlinger H, Streibel T, Suntz R, Bockhorn H. Influence of exhaust gas recirculation on soot formation in diffusion flames. Proc Combust Inst 2000;28:2643–9.
[22] Saleh HE. Experimental study on diesel engine nitrogen oxide reduction running with jojoba methyl ester by exhaust gas recirculation. Fuel 2009;88:1357–64.
[23] Maiboom A, Tauzia X, Hetet JF. Experimental study of various effects of exhaust gas recirculation (EGR) on combustion and emissions of an automotive direct injection diesel engine. Energy 2008;33:22–34.
[24] Kiplimo R, Tomita E, Kawahara N, Yokobe S. Effects of spray impingement, injection parameters, and EGR on the combustion and emission characteristics of a PCCI diesel engine. Appl Thermal Eng 2012;37:165–75.
[25] Nathan SS, Mallikarjuna JM, Ramesh A. Effects of charge temperature and exhaust gas re-circulation on combustion and emission characteristics of an acetylene fuelled HCCI engine. Fuel 2010;89:515–21.
[26] Peng H, Cui Y, Shi L, Deng K. Effects of exhaust gas recirculation (EGR) on combustion and emissions during cold start of direct injection (DI) diesel engine. Energy 2008;33:471–9.
[27] Shi L, Cui Y, Deng K, Peng H, Chen Y. Study of low emission homogeneous charge compression ignition (HCCI) engine using combined internal and external exhaust gas recirculation (EGR)". Energy 2006;31:2665–76.
[28] Ladommatos N, Abdelhalim SM, Zhao H, Hu Z. The effects of carbon dioxide in exhaust gas recirculation on diesel engine emission. Proc Inst Mech Eng D: J Automob Eng 1998;212:25–42.
[29] Beatrice C, Bertoli C, Cirillo NC, Giacomo ND, Innocente R. Influence of high EGR rate on emissions of a DI diesel engine. In: The 16th annual fall technical conference on the internal combustion engine division, Lafayette, USA; 1998.
[30] Haşimoğlu C, İçingür Y, Öğüt H. Dizel Motorlarında Egzoz Gazları Resirkülasyonunun (EGR) Motor Performansıve Egzoz Emisyonlarına Etkisinin Deneysel Analizi. Turk J Eng Environ Sci 2002;26:127–35 [in Turkish].
[31] Kökkülünk G, Gonca G, Ayhan V, Cesur I, Parlak A. Theoretical and experimental investigation of diesel engine with steam injection system

on performance and emission parameters. Appl Therm Eng 2013;54:161–70.
[32] G. Kökkülünk, G. Gonca and A. Parlak, The effects of design parameters on performance and NO emissions of steam injected diesel engine with exhaust gas recirculation Arab J Sci Eng, 39, 5, pp. 4119–4129.
[33] Needham JR, Nicol AJ, Such CH. Low emission heavy duty diesel engine for Europe. SAE Paper 1993-620-631.
[34] Ferguson R. Internal combustion engines-applied thermodynamic. New York (: John Wiley & Sons; 1986. pp. 180–7.
[35] Hohenberg G. Advanced approaches for heat transfer calculations. SAE Paper 1979-790825.
[36] Gonca G. Investigation of the effects of steam injection into the supercharged diesel engine with running miller cycle on performance and emissions. Yildiz Technical University; 2013. PhD thesis.
[37] Heywood JB. Internal combustion engine fundamentals. New York (: McGraw-Hill Inc.; 1988.
[38] Olikara C, Borman G. A computer program for calculating properties of equilibrium combustion products with some applications to the engines. SAE Paper 750468; 1975.
[39] Gonca G, Sahin B, Ust Y, Parlak A. A study on late intake valve closing miller cycled diesel engine,. Arab J Sci Eng 2013;38(2):383–93.
[40] Qi K, Feng L, Leng X, Du B, Long W. Simulation of quasi-dimensional combustion model for predicting diesel engine performance. Appl Math Model 2011;35:930–40.
[41] Bhaskar K, Nagarajan G, Sampath S. Optimization of FOME (fish oil methyl esters) blend and EGR (exhaust gas recirculation) for simultaneous control of NO_x and particulate matter emissions in diesel engines. Energy 2013;62:224–34.
[42] Zhang W, Chen Z, Shen Y, Shu G, Chen G, Xu B, et al. Influence of water emulsified diesel & oxygen-enriched air on diesel engine NO-smoke emissions and combustion characteristics. Energy 2013;55:369–77.
[43] Chang Y, Lee W, Wu TS, Wu C, Chen S. Use of water containing acetone–butanol–ethanol for NO_x–PM (nitrogen oxide-particulate matter) trade-off in the diesel engine fueled with biodiesel. Energy 2014;64:678–87.
[44] Gonca G, Sahin B, Ust Y, Parlak A, Safa A. Comparison of steam injected diesel engine and miller cycled diesel engine by using two zone combustion model. In: Proceedings of the 12th International Combustion Symposium vol. 16; 2012. pp. 115–25.
[45] Gonca G. Investigation of the effects of steam injection on performance and NO emissions of a diesel engine running with ethanol–diesel blend. Energy Convers Manage 2014;77:450–7.
[46] Sitkei G. Kraftstoffaufbereitung und Verbrennungbei Dieselmotoren. Berlin: Springer Verlag; 1964.